Urban Planning
2024 • Volume 9 • Article 8350
https://doi.org/10.17645/up.8350

cogitatio

ARTICLE

Open Access Journal

Urban Microclimate Impact on Vertical Building-Integrated Photovoltaic Panels

Max Spett, Kevin Lau, and Agatino Rizzo

Architecture Research Group, Luleå University of Technology, Sweden

Correspondence: Max Spett (max.spett@ltu.se)

Submitted: 8 March 2024 **Accepted:** 2 July 2024 **Published:** 29 August 2024

Issue: This article is part of the issue "Planning and Managing Climate and Energy Transitions in Ordinary Cities" edited by Agatino Rizzo (Luleå University of Technology), Aileen Aseron Espiritu (UiT The Arctic University of Norway), Jing Ma (Luleå University of Technology), Jannes Willems (University of Amsterdam), and Daan Bossuyt (Utrecht University), fully open access at https://doi.org/10.17645/up.i346

Abstract

The ongoing climate crisis and turbulence on the world stage has highlighted the need for sustainability and resilience in the development and maintenance of urban areas regarding climate comfort and energy access. Local production of green energy increases both the sustainability and resilience of an area. Traditionally, photovoltaic (PV) panels are deployed wherever the amount of sunlight is highest but lowering costs for PV panels makes them cost-effective even in colder climates. Within the broader umbrella of positive energy districts, façade mounted building-integrated PV panels in urban areas additionally present unique opportunities and challenges, as factors such as wind, solar irradiance, or nearby obstructions can have either a positive or negative effect on the performance of the PV panels. In this article, we aimed to answer the question: What factors inform the optimization of vertical PV panels? To answer this, we developed a method for the optimization of placement of PV panels. By building upon readily available weather data, local panel conditions were examined, and field-driven aggregation algorithm used to guide panel placement. Performance of the resulting panel configurations were then compared to a baseline case. Results indicate that our developed method helped mitigate negative impacts of the aforementioned factors, and often improved performance over baseline.

Keywords

building envelope; building-integrated photovoltaic panels; field-driven aggregation; form finding; positive energy districts

1. Introduction

The decarbonization of the economy, as a response to climate change, poses significant challenges to the housing sector. Research estimates suggest that the housing sector alone contributes a substantial amount of CO^2 emissions annually, accounting for approximately 30% of total global greenhouse gas (GHG) emissions (Swedish Energy Agency, 2020). This places it alongside industry and transportation as the principal sources of environmental impact (Nejat et al., 2015). These figures highlight the urgent need for targeted policies and innovations in these sectors to mitigate their environmental footprint. In response to the pressing need for sustainable development, the United Nations introduced the Sustainable Development Goals (SDGs) and facilitated the Paris Agreement in 2015. These initiatives represent a global commitment to transforming economic activities by significantly reducing GHG emissions. The SDGs and the Paris Agreement underscore the collective acknowledgement of climate change's threats and the imperative for immediate and coordinated actions to ensure a sustainable future (United Nations, 2023).

This pursuit is critical for maintaining Sweden's status as an advanced industrialized economy, which historically has relied on cheap and reliable energy sources, including hydro power, nuclear, and various non-renewable options. However, the global push towards sustainable development, spearheaded by the SDGs and the Paris Agreement, has accelerated Sweden's shift towards greener energy sources. By 2022, Sweden had already made significant progress, with 66% of its energy consumption coming from renewable sources, a stark contrast to the European Union average of 23%, according to Eurostat (2023). This transition is increasingly characterized by investments in wind energy, photovoltaics (PVs), and hydrogen for energy storage, marking a pivotal shift from its historical energy mix towards a future powered by renewable energy, setting a commendable example for nations worldwide. At the urban scale, since 2018 the EU has directed working groups and funding to transform existing urban areas into positive energy districts (Joint Research Center, 2018), that is, neighborhoods that produce more energy that they need over a calendar year.

One of the important factors to achieve this target is to localize PV energy production by integrating it within urban and building contexts. Urban environments, characterized by their density and fragmented nature, present a stark contrast to the expansive openness of typical solar parks, necessitating innovative approaches for PV panel integration across diverse urban scenarios (Kalogirou, 2013; Savvides et al., 2024; Vassiliades et al., 2023). Particularly in high-latitude countries, the potential for vertical façades to harness solar energy has been recognized (O'Hegarty et al., 2016). However, both in practice and scholarly research, examples of PV panel integration in building façades remain scarce. This highlights a critical need for the development of new methodologies that not only optimize the technical performance of PV panel technologies but also consider their aesthetic integration within urban landscapes.

In this article, we explore the critical role of building-integrated PV (BIPV) panels within the broader framework of urban climate mitigation strategies, particularly emphasizing its importance in reducing GHG emissions in the housing sector. We do so by having as a case study an ordinary middle size city in Sweden, Luleå. 65% of the total population in Sweden lives in middle and small cities (Rizzo et al., 2020). At the same time, these cities have the least amount of (both human and capital) resources to achieve Sweden national target of 100% electricity generated by renewable energy sources by 2040. By tracing the evolution and development of BIPV panels, we underscore their potential as a key element in achieving energy sustainability and climate resilience. Our investigation specifically focuses on the application of BIPV panels

in façades, an area of significant relevance in high-latitude regions where solar radiation can be captured both in vertical and horizontal planes. Central to our analysis is the need for optimizing the configuration of BIPV panels in these systems to enhance their efficiency and aesthetic integration into urban architecture. This article aims to provide a comprehensive examination of the technical and environmental aspects of BIPV panel integration, advocating for optimized configurations as essential to leveraging the full potential of BIPV panel façades in contributing to the reduction of GHG emissions and the promotion of a green transition in urban environments.

Differences in temperatures, sun paths, and urban morphology mean that conditions for BIPV panel systems differ in different locations, and strategies need to account for local conditions to achieve optimal performance. Freitas et al. (2020) assessed BIPV panel performance in Brasilia, Brazil. They found that surrounding geometry presented noticeable shadowing on neighboring buildings and found that BIPV panel roof applications outperformed BIPV panels applied on façades. They also emphasized the need for panel cooling in warmer climates. Shekar et al. (2023) assessed the impact of tilt angle on the performance of PV panels in the subarctic city of Oulu in Northern Finland. They found that their vertical PV panel setup performed better than their rooftop panels during autumn and winter. The vertical PV panels were also unaffected by snow, unlike the rooftop inclined panels. Numerous methods to optimize PV panel deployment for local conditions have been proposed. Several studies have focused on methods for the optimization of building surfaces for PV panels, often focusing on building envelope morphology. Shirazi et al. (2019) optimized PV panel placement on roofs and façades in Tehran, Iran, from a cost/benefit point of view. They considered the impact of PV panel angle and placement density, although the panels were arranged in a more traditional, rectangular grid. Vulkan et al. (2018) assessed the solar potential of façades in Rishon LeZion, Israel, when accounting for the impact of shadows. They found that while low-rise buildings had high total solar exposure on both roofs and south-facing façades, high-rises solar exposure was mostly concentrated on their façades, due to the high façade area and low roof area. While the study took buildings' façade features such as windows into account, this was expressed as a ratio of total façade area, rather than actual positioning of individual elements. Bomfim and Tavares (2019) used meteorological data to optimize façade construction for PV deployment. They compared the angles between points on the façade and solar angles, optimizing the façade angles for use as a substrate for PV panels. Several methods deployed evolutionary and genetic algorithms to optimize solar gain. Esfahani et al. (2021) optimized residential building roof shapes for high solar gain potential. They deployed an evolutionary algorithm to find optimal roof tilt, shape, azimuth, and building aspect ratios for sun exposure. Walker et al. (2019) utilized genetic algorithms to optimize placement of thin-film copper-indium-gallium-selenide cells on a parametric, non-planar roof, focusing both on panel placement and interconnection.

By contrast, our method focused on optimizing placement of panels on existing building façades. We have developed a method for using differences in temperatures, shade, and urban morphology present in a subarctic city in Northern Sweden as a generator for finding optimized, non-gridded, panel placements. While aspects of our area of interest have been explored, as in the aforementioned studies, to the authors' knowledge combinations as in our specific case remain relatively unexplored. Specifically, we set out to answer the following question: What factors inform the optimization of vertical PV panels in a typical middle size city urban configuration in Sweden? We were also interested in exploring how microclimate conditions affect the performance of vertical PV panels and whether the morphology of cities affect how PV panel configurations perform.

In this article, we introduced a novel method crafted to optimize the placement of vertical PV panels across various usage scenarios in Section 2. The approach leveraged an algorithm developed within the Grasshopper platform, tailored to assess and enhance the performance of BIPV panel systems. In Section 3, the algorithm was applied to examine and contrast different scenarios, considering usage patterns and local environmental conditions. Section 4 delved into a discussion where we synthesized our findings from Section 3 to directly address our central research question. Here, we articulated the role and influence of the investigated factors on façade optimization and BIPV panel efficiency. We have concluded with a summary of our findings, outlining their implications for future research in sustainable urban design and renewable energy integration.

2. Methods

2.1. Site and Weather Data

The methodology was evaluated in Luleå, a city situated in Sweden's northern region (Figure 1). As of the end of 2020, Luleå had a population of 49,123 (SCB, 2021) and serves as the administrative center of Norrbotten County. Characterized by its subarctic climate, Luleå falls within the Köppen Dfc climate zone. For this study's purpose, two multi-story residential buildings in the city were chosen as test sites, both presumed to be constructed in the latter part of the 20th century. The first building, located in the Örnäset suburb, stands at six stories. The selected testing surface on its façade faces 127° southeast and is partially covered by windows. While the façade covers an estimated 187m^2 on the selected building side, the planar subset used covers 102m^2 and the largest subsection without windows 45m^2. The surrounding area exhibits medium density housing, predominantly three-story buildings. The second building is situated in Luleå's central district, rising four stories high. Its testing façade faces 166° south and, similar to the Örnäset site,

Figure 1. Map of central Luleå. The respective host buildings are highlighted in red. The city center location is situated to the west and Örnäset to the east.

features partial window obstructions. The façade covers an estimated 108m^2. The largest subsection without windows covers 45m^2. The central area is denser, with narrower streets and a greater variety of building heights.

For weather data, we utilized the Typical Meteorological Year (TMY) dataset from the Climate.Onebuilding.org project, presented in the EnergyPlus Weather (EPW) file format. The primary data collection point was Luleå-Kallax Airport, located at latitude 65.5430 and longitude 22.1240. The airport is located 4.9 km southwest from Örnäset test site and 4.2 km from the city center test site. The two sites are located 2.2 km apart.

2.2. Model Construction

Our methodology primarily utilizes the Rhinoceros 3D CAD modeling software and Grasshopper, a visual programming language and environment tailored for Rhinoceros. Renowned for its robust geometric modeling capabilities, Grasshopper is extensively employed by architects, engineers, and urban planners. It benefits from a vast ecosystem of third-party plugins, including a variety of energy simulation tools that are particularly relevant to our study. Additionally, for data processing and final evaluation, we employed Pandas, a comprehensive data analysis library, and pvlib, a PV performance assessment toolbox, in Python. This combination of tools enables a sophisticated approach to modeling, simulation, and analysis, facilitating the optimization of vertical PV panel placement within building façades.

Our methodology unfolds through a structured series of steps designed to construct and analyze our model comprehensively:

1. *Model Construction*: Initially, we create detailed models of buildings and their surrounding neighborhoods. This process leverages open mapping data verified by field observation to ensure accuracy of the geometry. Alongside, we acquire TMY data to simulate local weather conditions accurately.
2. *Local Conditions Synthesis*: Utilizing the foundational data from the first step, we conduct simulations and calculations to encapsulate the local environmental conditions comprehensively. This step is crucial for understanding the specific context in which the PV installations will operate.
3. *PV Placement Optimization*: The insights gained from the synthesis of local conditions are then applied to optimize the placement of tiled PV panels. This optimization process uses a field-driven aggregation approach, guided by a set of weights, to determine the most effective arrangement for energy generation.
4. *Performance Evaluation*: Finally, we assess the energy performance of the PV panels in their optimized arrangement. This evaluation involves comparing the optimized setup against a baseline scenario, where standard panels are used instead. Through this comparative analysis, we aim to quantify the benefits of our optimized placement strategy in terms of increased energy efficiency and potential for renewable energy generation.

2.2.1. Construction of Building Neighborhood

Building outline data was obtained through manual download from the crowd-sourced open mapping platform OpenStreetMap (2017), subsequently processed using the Elk plugin for data parsing.

OpenStreetMap provides building data as a collection of points that delineate the building's two-dimensional footprint in the WGS 84 standard, accompanied by various metadata elements. This metadata may include details on the building's height, number of floors, or in some cases, neither. To transition from two-dimensional footprints to three-dimensional models, we employed the provided height data directly when available. In instances where only the number of floors was specified, we calculated height estimates by multiplying the number of floors by 2.7 m. For buildings lacking both height and floor count information, a default single-story height of 2.7 m or multi-story height of 8.1 m was assumed, depending on how high the average building in the neighborhood was determined to be. These procedures enabled the extrusion of building footprints to their corresponding heights, resulting in a comprehensive set of three-dimensional building volumes.

Following the automated generation of the neighborhood's building models, structures in proximity to the designated area for PV panel installation underwent manual verification and adjustment. This process involved comparing the generated building models to photographs captured during site visits. Discrepancies, such as a single modeled outline inaccurately representing adjacent buildings or significant deviations between the model and the actual building's appearance, prompted corrections. These adjustments were meticulously carried out using the modeling capabilities of Rhinoceros, ensuring that the digital representations closely matched the real-world conditions.

2.2.2. Construction of Analytical Model

The building designated for PV panel integration received a higher level of detail in its modeling compared to the surrounding structures. This detailed modeling was achieved through manual techniques within Rhinoceros. We focused on accurately modeling a typical storey, under the assumption that each subsequent storey would mirror this template, except for significant deviations. The standard height for each storey was set at 2.7 m. Estimations for window positions and configurations were derived from photographic evidence, while the layout and dimensions of the apartments were also approximated. This typical story model was then replicated for each floor, culminating in the construction of the building to its full intended height.

To precisely control the placement of PV panels and ensure they are confined to specific sections of the façade, a particular surface area of the façade was chosen to act as the base for panel installation. This chosen area, referred to as the "crawling surface," was extracted from the vertical sections of the building's model. It spanned from the ground level to the building's roof, incorporating openings where windows are located to exclude these sections. Utilizing this surface, we then engaged the Wasp plugin (Rossi, 2021) to generate a "Wasp Field" along with a corresponding point grid. This grid was strategically positioned 20 cm from the façade, with grid points spaced 25 cm apart, effectively enveloping the designated surface area for PV panel application.

2.2.3. Derived Values

The Wasp plugin serves as a sophisticated combinatorial toolkit designed for crafting complex geometric configurations. By defining a series of geometries alongside rules for their combination—specifying permissible connections between parts—Wasp orchestrates the assembly of these geometries into cohesive

aggregations. These assemblies can be generated through stochastic processes or be directed by specific fields, also incorporating collision detection to prevent geometric overlaps. In our approach, we chose to guide the aggregation of PV panels using a method influenced by fields. To this end, we established three fields to steer the placement process effectively. An occupancy grid field was designed to ensure that panels do not obstruct windows and doors, maintaining clearances. Another field was derived from the shadow patterns on the building, advising the algorithm to avoid areas that receive less sunlight. Finally, a wind strength field based on computational fluid dynamics (CFD) was constructed to inform the algorithm about local wind conditions. We limited the aggregation to a two-dimensional plane close to the building walls to maintain coherence with the architectural structure. This algorithm evaluates points within the field, favoring locations with higher value assignments for panel placement, thus optimizing their positioning.

To aid in this optimization, we developed a building occupancy grid (BOG) based on the crawling surface. Each point in the point grid was evaluated in relation to the façade. Points directly in front of where PV panels could be placed were assigned a value of 1, indicating optimal placement zones, whereas points coinciding with non-panel areas, such as those in front of windows, were assigned a value of 0, signaling exclusion from panel placement.

2.3. Microclimate Simulation

The Ladybug plugin suite was employed to trace the sun's path across the sky for the given location over the course of a year, enabling us to simulate the impact of shadowing from surrounding buildings on the building façade. This simulation produced a mesh overlaying the building façade, each mesh point representing the cumulative hours of direct sunlight received annually. Points within our established point grid were then mapped to the nearest mesh point values, assimilating the sunlight exposure data. These values were subsequently normalized by dividing them by the total annual sun-over-horizon hours, which amounted to 4,556 hours in our study area. This normalization process yielded sun exposure ratios (SER) for each grid point, quantitatively expressing the relative solar exposure across the façade.

A CFD analysis was conducted to assess local wind patterns around the building and its immediate surroundings, utilizing the building models without incorporating ground mesh or vegetation in the simulation setup. This study utilized the Eddy 3D plugin (Kastner & Dogan, 2021), which employs the 2017 version of BlueCFD, a distribution of OpenFOAM, for its simulations. The simulation domain was configured as a cylinder, with an inner rectangular area measuring 200 m on each side and the outer cylinder dimensions set at a diameter of 450 m and a height of 113 m, with a uniform block size of 3 m throughout. The meshing process was executed using a snappy mesh technique, assigning a meshing precision of 3 for the buildings and their edges, while the planar ground surface received a precision level of 2, and the bounding box was set at 0. Utilizing the Shear Stress Transport k-ω model for turbulence, along with finely tuned relaxation factors and control settings for the solution and algorithm, the wind conditions were simulated across eight directions, corresponding to the cardinal and intercardinal points, at a reference height of 10 m and with a surface roughness assumption of 1 m. Each of the eight simulations ran for 1,024 iterations, reaching a loosely convergent state with residuals for all wind velocity components (Ux, Uy, Uz) falling below 10^{-4} for all directions, except for a slightly higher residual of 1.01556×10^{-4} observed in the eastern wind simulation for the city center case.

Wind velocity data derived from the CFD simulations were analyzed at each point within the grid to calculate their annual wind factor. This calculation was facilitated by the Wind Factors component within Eddy3D. The process involves matching each hourly wind data point from the EPW file to the nearest wind direction simulated and adjusting the data to align with the simulated wind velocities. This approach allows for the generation of an estimated wind factor for each grid point for every hour of the year. The compiled data forms a comprehensive matrix indicating the hourly estimated wind factors for each test point throughout the year. To synthesize this data, the annual average was computed across the matrix, producing a condensed matrix that presents the yearly mean wind factors (YMWF) for each grid point, offering a streamlined overview of wind exposure at each location over the course of the year.

The resulting BOG, SER, and YMWF were each weighted, i.e., multiplied by a weight between 0 and 1, and then summed together for each point. This combined field was then used to inform the aggregator for where to place tiles in the following step.

For both locations, base cases were constructed. The base cases consisted of 14 regular PV panels, placed in grids on the windowless portion of the façades. The panels were modelled as rectangles and would later serve as a reference to compare panel performance against. For our method, the panels were modelled as polygonal shapes. For simplicity, regular pentagons, each ¼th the area of a base case panel, were selected as the aggregating shape. While shapes other than pentagons can be used, we selected pentagons as they do not tile the plane, which combined with our selected aggregation method create diverse designs and avoid obstructing windows. For both locations, a total of 57 panels were placed and the total as to closely match the total area of the base case. Starting points for the aggregations were determined experimentally, with each starting in the upper part of the windowless area. An initial pentagon was placed, after which the pentagons were set to aggregate over the selected surface, guided by the field. The aggregation was performed by the field-driven aggregation component provided by the Wasp plugin. The aggregator placed panels edge-to-edge, sampling the grid, and placing the panel at the most beneficial location. This was repeated until all 57 panels were placed. By varying the weighting given to the BOG, SER, and YMWF, varying placements of panels can be achieved. To test different configurations, three different sets of weightings were tested. In all cases, the BOG weighting was set to 0.5, while in Test Case 1 SER was set to 0.0 and YMWF to 1.0, in Test Case 3 the opposite, with SER set to 1.0 and YMWF to 0.0. For each location, a case which balanced the traits between the extremes were created and named Test Case 2. For Örnäset, SER was set to 0.95 and YMWF to 0.05, while for the city center, SER was set to 0.6 and YMWF to 0.4 (see Table 1). The weightings were derived experimentally. In total, 8 panel arrangements were constructed, i.e., 4 per site, each consisting of 1 base case and 3 test cases using our method.

To facilitate comparison between panel arrangements, the panels in the test cases were substituted with panels identical to the ones used in the base case. Positions for these impostor panels were determined by clustering. The centroids of the source panels were divided into 14 clusters using k-means clustering, as

Table 1. Weightings of panel generation test cases.

	Test Case 1	Test Case 2: City Center	Test Case 2: Örnäset	Test Case 3
BOG	0.5	0.5	0.5	0.5
SER	0.0	0.6	0.95	1.0
YMWF	1.0	0.4	0.05	0.0

implemented by the NGon plugin suite for Grasshopper (Vestartas & Rad, 2021). At each respective center, impostor panels were placed and evaluated. The wind simulations performed at both locations were again sampled at the panels' center points and the annual wind factors were calculated, although the results were not averaged at this point. The amount of sun exposure for each panel was calculated, with data for whether the panel was considered in sunlight or shaded by neighboring buildings being recorded for each hour throughout the year (Figures 2 and 3).

The performance of test panels was evaluated against a reference case using the Python programming language using Pandas and pvlib. pvlib is a toolbox providing various tools for assessing PV energy systems (Holmgren et al., 2018, 2023). pvlib has been validated against real-world measurements by Deville et al. (2024), in which all models performed well, the authors finding the average normalized mean bias error to be within ±2.3% of the real-world measurements. It makes available databases of both Sandia PV panel modules and CEC inverters. A modern and dimensionally suitable panel was selected from the Sandia database, U300 Black from Silevo Triex. The inverter was selected by filtering the CEC Inverter database.

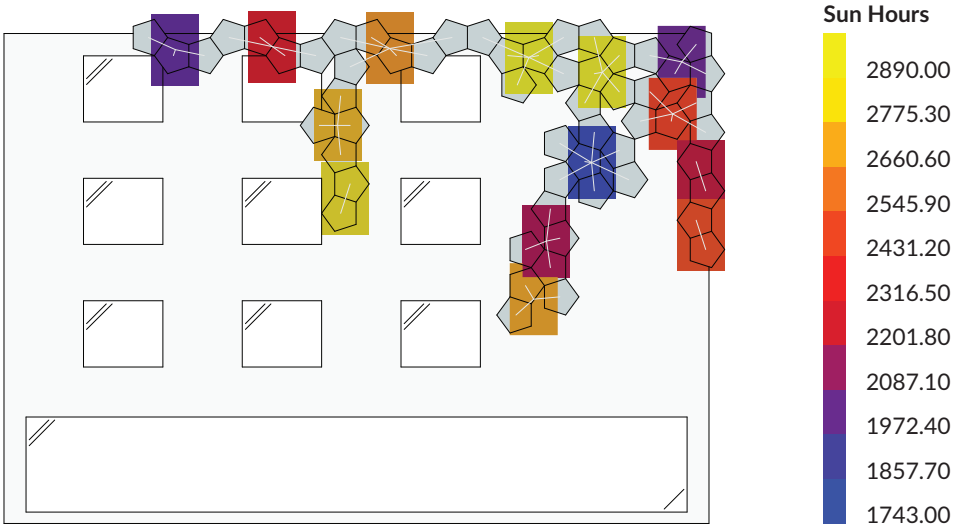

Figure 2. Sun exposure by panel and diagrammatic drawing of façade and panel aggregation, as well as the k-means clustering. While the panels overlap, they are separate in the simulation. City Center Test Case 2.

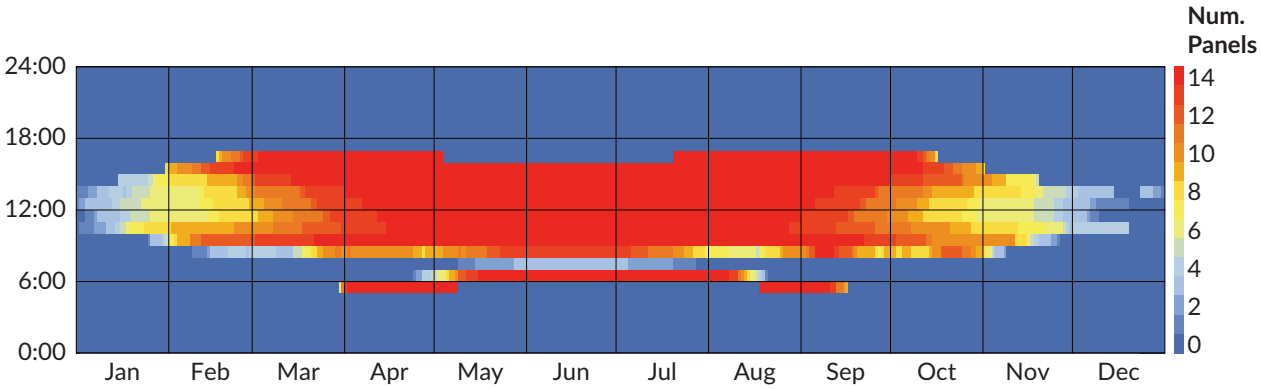

Figure 3. Number of panels with direct exposure to the sun throughout the year. Notably, the panels do not receive direct sunlight between 08:00 and 09:00 for a large portion of the year due to a nearby multi-storey building blocking the sun. City Center Test Case 2.

Inverters with an AC output of 240 V was selected, then further filtered by selecting inverters where the AC output was achieved with a voltage either matching or exceeding (by a maximum of 25 V) the peak voltage output of the panel. Finally, the inverter with the lowest DC power requirement before outputting AC power was selected, the Sunteams 1500 from Beijing Kinglong New Energy Technology. The inverter also has a low night tare, which is important in the dark winter months. The vertical PV panel were assumed to be freestanding, and both the reference and test panels were set up with one inverter per panel. The altitude of the panels was set to their height in the model, plus 8 m. Using air temperature, direct normal irradiance, global horizontal irradiance, and diffuse horizontal irradiance values for the whole TMY from the EPW data, the panels were set up for evaluation in pvlib. A dedicated weather profile was constructed for each panel. DNI, GHI, and DHI values were modulated by whether the particular panel was considered to be shaded for a given hour, with values being set to 0 if panels were in shade. The air temperature and albedo data were applied verbatim while the calculated annual wind factors were used as wind speed. The TMY performance of each panel was then simulated in turn, and the results aggregated.

3. Results

To facilitate comparison, the hottest, coldest, stalest (least windy), windiest, and sunniest weeks in the typical mean year data were identified. As the TMY data is an amalgamation of several years' data, the year was assumed to start on a Monday, as was the definition of "week." The mean of each week's weather was used as a basis for the criteria, and the 31st of December was ignored in terms of week selection in order to only analyze full weeks. Wind chill effect was not considered, i.e., only air temperature was considered for the warmest and coldest weeks. The coldest week was week 4 between the 22nd and 28th of February. Temperatures ranged between −26 and 0 °C, the mean wind speed was 3.63 m/s, and the mean of the sum of solar irradiance values was 30.86 Wh/m^2. The hottest week was week 30 in the middle of summer, between the 23rd and 29th of July. Temperatures varied between +10 and +24 °C, mean wind speed was 3.08 m/s, and solar irradiance 651.21 Wh/m^2. The windiest week was in spring, week 43 between the 22nd and 28th of October. Temperatures varied between −8 and +3 °C, mean wind speed was 5.77 m/s, and mean irradiance 53.06 Wh/m^2. The stalest week was week 9, between the 26th of February and 4th of March. Temperatures varied between −22 and −1 °C, mean wind speed was 2.13 m/s, and mean irradiance 143.47 Wh/m^2. The sunniest week was week 22 in early summer, between the 28th of May and the 3rd of June. Despite being the week with the largest amount of sun radiation, temperatures were still relatively low, ranging between +2 and +15 °C. The mean wind speed was also relatively high, at 5.41 m/s. The mean irradiance was 68.52 Wh/m^2. The weather is summarized in Table 2 and Figure 4.

Table 2. Representative weather weeks from the TMY.

Week Type	Week Range	Temperature Range (°C)	Mean Wind Speed (m/s)	Mean Irradiance (Wh/m^2)
Coldest Week	Week 04: Jan 22–Jan 28	−26–0	3.63	30.86
Hottest Week	Week 30: Jul 23–Jul 29	+10–+24	3.08	612.90
Windiest Week	Week 43: Oct 22–Oct 28	−8–+3	5.77	53.06
Stalest Week	Week 09: Feb 26–Mar 04	−22–−1	2.13	143.47
Sunniest Week	Week 22: May 28–Jun 03	+2–+15	5.41	768.52
Whole Year	Jan 01–Dec 31	−28–+26	3.57	292.97

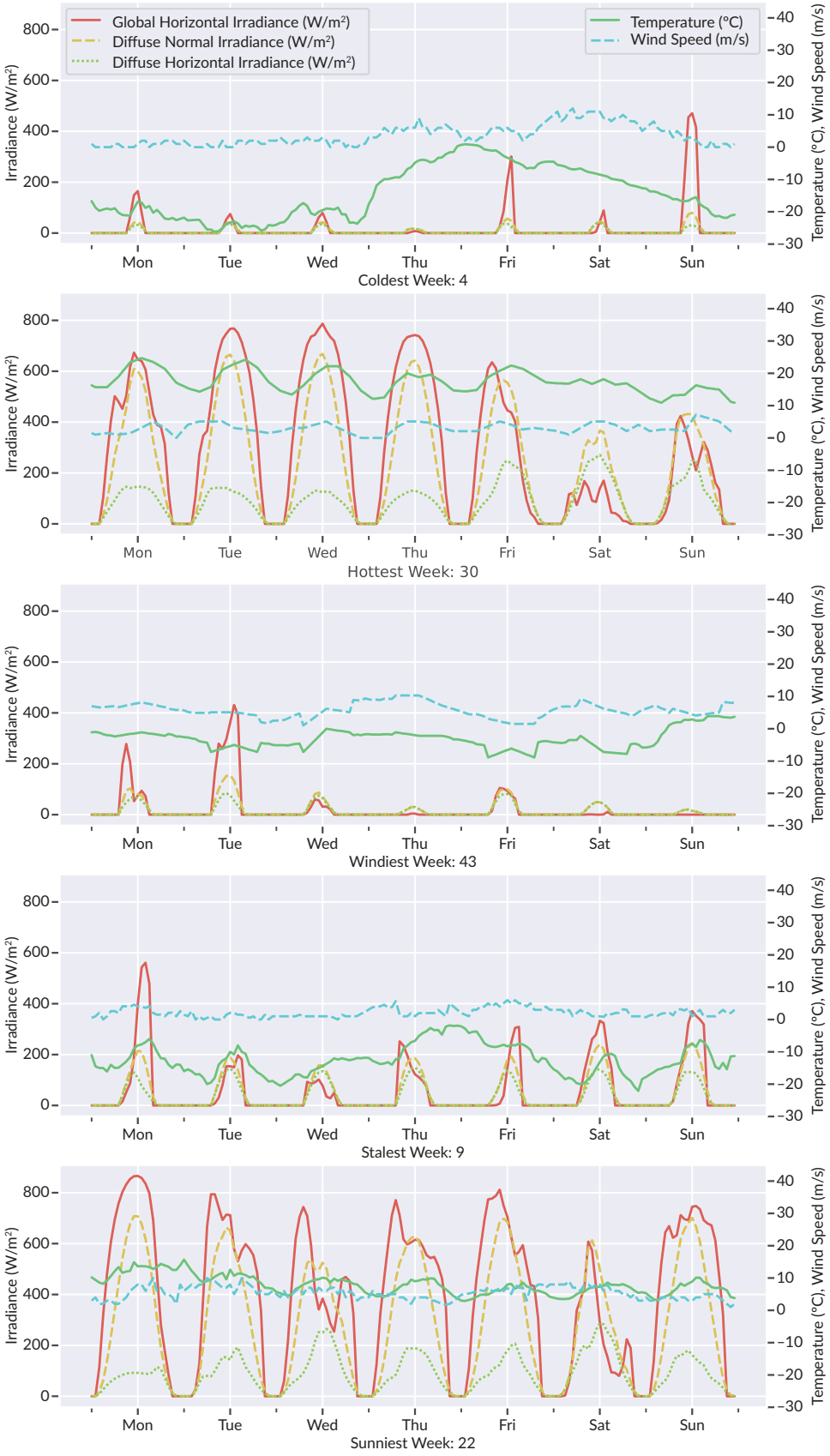

Figure 4. Weather during the representative weeks.

The climate conditions affected the performance of all panel configurations, but not in a uniform manner. The sunniest week, week 22 between May and June, was the most productive period for all panel configurations, followed by the hottest week, week 30 in July. Compared to the sunniest and hottest weeks, the week with the lowest mean wind speed, week 9 in February, performed less well, with all panel configurations underperforming. The coldest and windiest weeks of the year were week 4 in January and 43 in October, where no panel performed particularly well. The vertical PV panels in Örnäset generally performed better than their counterparts in the city center, with the exceptions of test panel 3 in the city center outperforming Örnäset during the coldest week, test panel configurations 2 and 3 performing better than the Örnäset panels during the windiest and stalest weeks, and the reference panels performing better during the stalest week. The different test panel configurations showed minimal deviation in performance and temperature from the reference panels in Örnäset, indicating little variance during all testing periods. In contrast, the panel configurations in the city center demonstrated significant performance variability, with notable differences across all test periods. Throughout the year, the panels in Örnäset consistently performed better, except for test panel configuration 3 in the city center, which exhibited the best annual performance. PV cell temperatures exhibited less variations than the panel performance. For Örnäset, temperatures remained consistent across all panel configurations. Cell temperatures somewhat varied more in the city center, with test panel configuration 1 consistently being the coolest and configuration 3 being the warmest. The panel configurations are summarized in Table 3. Figure 5 shows the performance of the city center panels configurations for each week and Figure 6 shows the equivalent performance for Örnäset.

Table 3. PV panel performance.

		Week Type	Coldest	Hottest	Windiest	Stalest	Sunniest	Year
Aggr. AC Output (kWh)	Örnäset	Reference Panels	−0.46	78.50	5.72	24.90	104.27	2,259.20
		Test Panels 1	−0.51	78.54	5.55	24.71	104.30	2,258.31
		Test Panels 2	−0.45	78.50	5.72	24.97	104.27	2,259.75
		Test Panels 3	−0.45	78.50	5.72	24.97	104.29	2,260.39
	City Center	Reference Panels	−0.80	66.68	4.29	26.43	81.58	2,060.62
		Test Panels 1	−0.88	65.29	3.23	17.51	81.33	1,821.35
		Test Panels 2	−0.53	68.44	6.58	31.62	83.54	2,169.02
		Test Panels 3	−0.17	71.48	9.40	43.40	85.42	2,343.69
Mean Cell Temp (°C)	Örnäset	Reference Panels	−13.76	22.74	−2.47	−10.52	14.39	5.32
		Test Panels 1	−13.81	22.71	−2.50	−10.56	14.37	5.29
		Test Panels 2	−13.75	22.74	−2.44	−10.51	14.39	5.31
		Test Panels 3	−13.75	22.73	−2.44	−10.51	14.37	5.30
	City Center	Reference Panels	−14.26	22.20	−2.60	−10.69	13.21	5.05
		Test Panels 1	−14.19	22.05	−2.73	−11.24	13.14	4.75
		Test Panels 2	−13.96	22.27	−2.44	−10.37	13.32	5.19
		Test Panels 3	−13.74	22.49	−2.22	−9.68	13.43	5.41

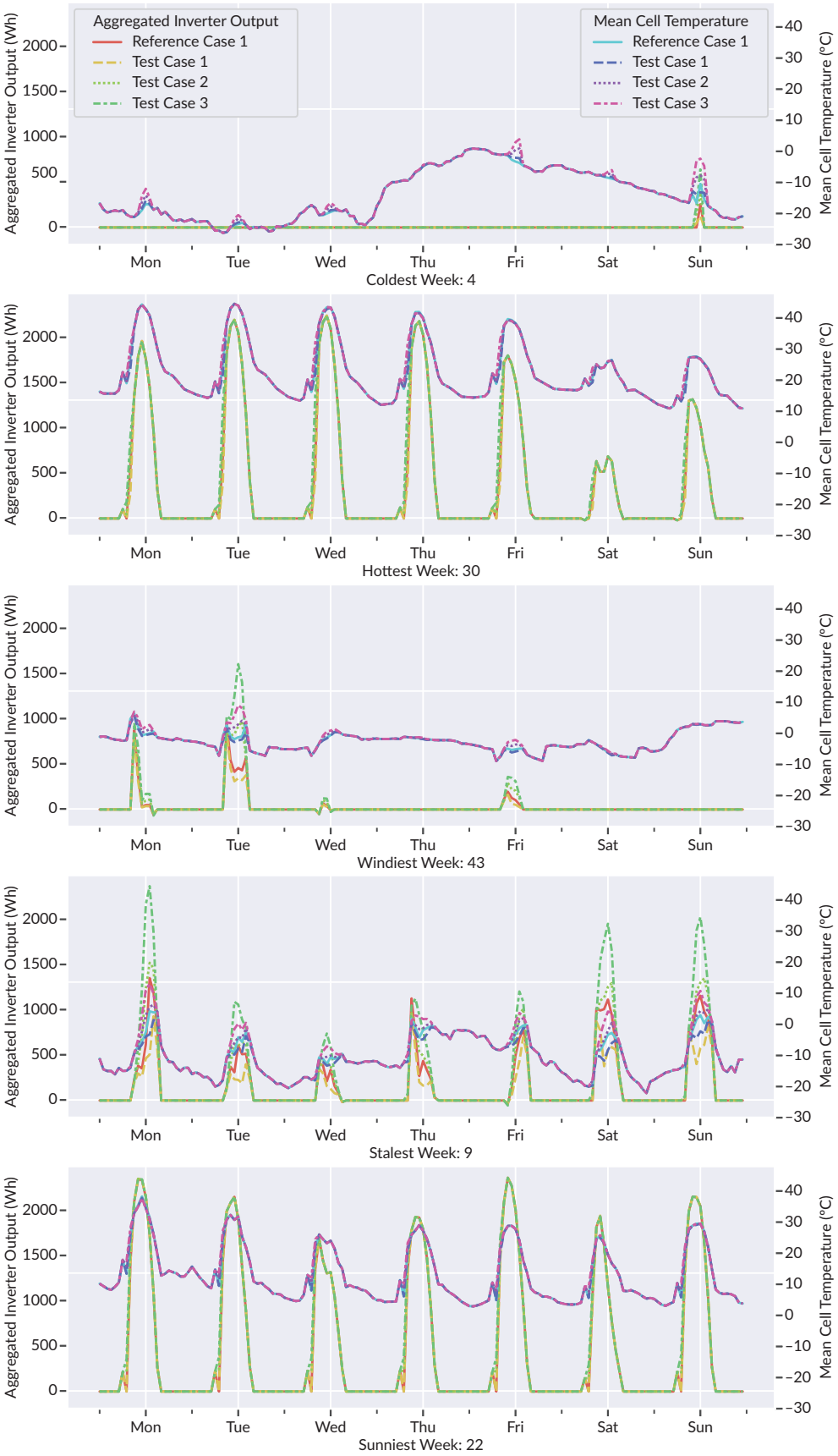

Figure 5. City center PV panel configuration performance.

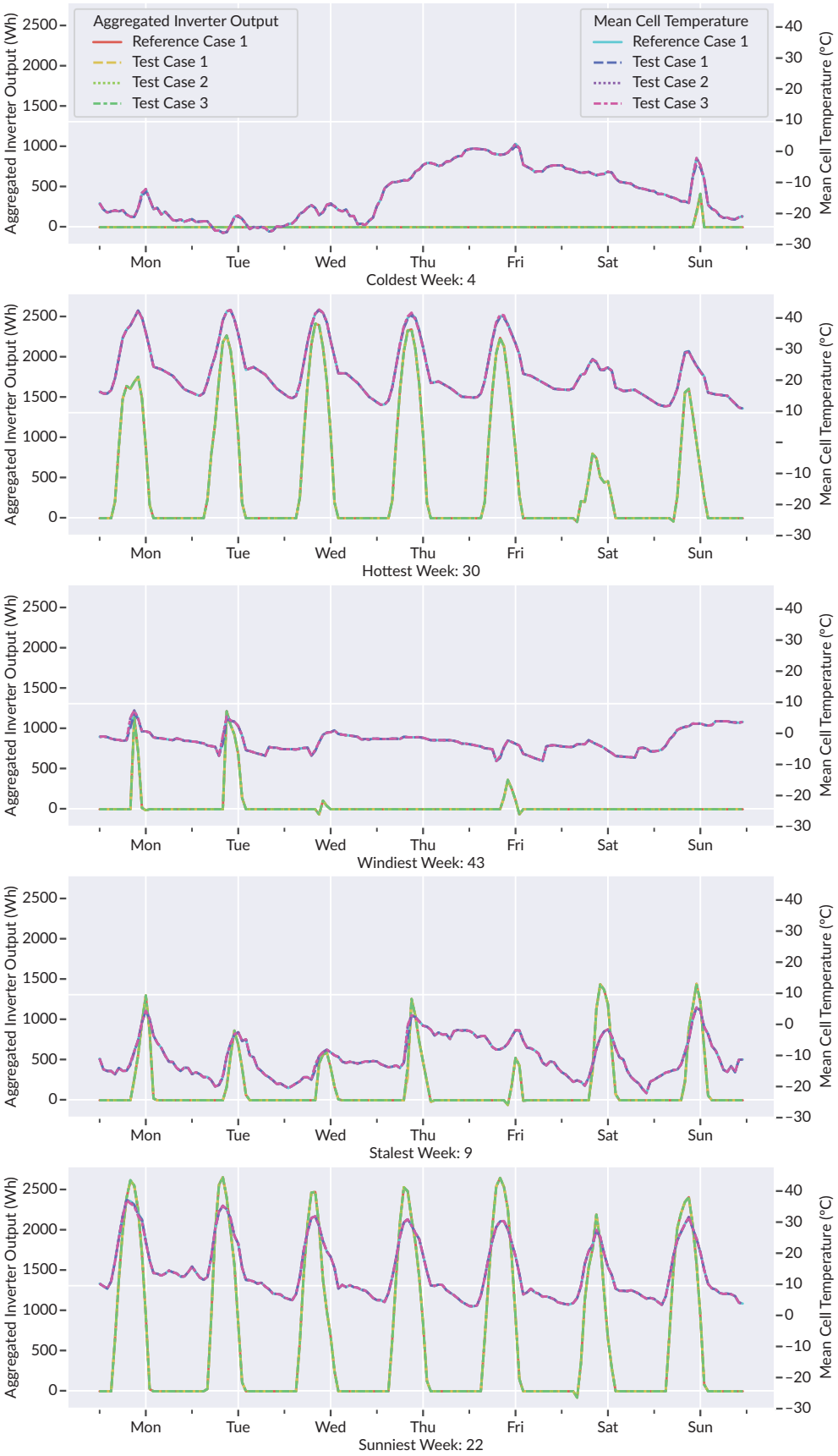

Figure 6. Örnäset PV panel configuration performance.

4. Discussion and Conclusions

In this article, we introduced a novel method for the optimization of the positioning of PV panels on building façades. In order to transform existing urban areas into positive energy districts there is a need to use all the available building surface for the installation of PV panels. In Nordic countries, this means to use façades as well as the solar azimuth is quite low. However, not all of the possible usable surface can generate appreciable amount of energy as well as there are important construction and architectural implications to consider when upscaling PV coverage in urban areas. Using publicly available cartographic and weather data, models for two urban scenarios in the subarctic city of Luleå, Sweden, were constructed. Microclimate simulation of wind, coupled with and façade obstruction provided three-dimensional fields representing each factor. The factors were then weighted to create three scenarios. Guided by these three fields, the panels were aggregated into three configurations, which in turn were clustered into a set of impostor panels for the sake of comparison. The performance of the panels was evaluated and compared to a typical, gridded configuration. We found that the configuration of the panels had an impact on their performance, with some configurations performing above the typical gridded configuration, and others below.

Our initial question was: What factors inform the optimization of vertical PV panels in a typical middle size city urban configuration in Sweden? Based on our simulation models we suggest that local conditions such as microclimate and city morphology do seem to have an effect on how different configurations of BIPV panels perform, although the complexities of the results suggest that there is no one optimal solution. The results indicate that alternative configurations of PV panels could yield energy gains in the right conditions. It also showed that evaluation is of importance, as not every design was an improvement over the base case. In the city center, test panel configurations 2 and 3 outperformed the reference case in all scenarios, as well as throughout the year. Configuration 3 also had the best yearly performance of any panel, irrespective of location. By contrast, test panel configuration 1 underperformed in all cases. As Test Case 1 prioritized panel aggregation towards areas with high mean wind factor to the detriment to areas with high sun exposure, this could indicate that the sun exposure factor is a better indicator for PV panel performance, especially since test panel configuration 3, which prioritized sun exposure, performed better than both the reference and other test panel configurations.

The morphology of the surrounding area seems to play a large role in the performance of the panel arrangements. The relatively minor differences in performance between well-performing test cases in Örnäset and the larger differences between panel performance in the city center indicates that panel arrangement optimization is potentially more beneficial in morphologically more difficult urban settings. That the third test arrangement in the otherwise less performant city center had the most efficient yearly performance is promising, indicating that the application of our methods could lead to more efficient panel arrangements, even in already optimal cases. The flexibility of our method allows it to be used by designers and decision makers to explore design spaces and develop informed understandings for the viability of panel configurations. The novel approach towards shapes lets designers reevaluate how PV panels can look. Future studies would benefit from an evaluation of panel aesthetics. In a survey by Bao et al. (2017), participants indicated that they were willing to pay more for aesthetically pleasing panels. The survey also showed that more aesthetically pleasing panels are preferred by testing groups, especially when seen in context to the building they are installed to, although the study showed that less visually intrusive panels were preferred.

While PV panel shapes were limited to one in this study, future research could expand upon the range of selected shapes, as well as the use of multiple shapes. For our study, we chose to use pentagons. As pentagons do not tile the plane, their manufacture would likely be less efficient than tilable shapes such as triangles and especially rectangles. Another main limitation is due to the lack of empirical testing of our model. We plan to conduct future experiments in the following steps of our ongoing projects. Although currently an involved process, our method has the potential to be highly automated. Future research could streamline the presentation and user experience, enabling our method to be used by decision makers and non-researchers to inform urban planning and architectural developments.

Furthermore, Ricci et al. (2020) compared the accuracy of turbulence models in the CFD software Gambit in comparison to a 1:300 scale wind tunnel model of Quartie La Venezia, Livorno, Italy. While the authors found the majority of models, including the Shear Stress Transport k-□model used in this article, to have a similar qualitative wind flows in the urban canopy layer, they found that all models had issues with flows around and downstream obstructions such as buildings. Therefore, future studies could benefit from local verification of wind conditions to ensure accuracy. Additionally, as our method presented in this article is novel, future research could benefit from verifying PV panel performance in real test cases.

Acknowledgments

Map data copyrighted OpenStreetMap contributors and available from https://www.openstreetmap.org. The ChatGPT-based LLM Consensus was used for finding literature relevant to the topic: https://chatgpt.com/g/g-bo0FiWLY7-consensus.

Funding

This project was supported by Formas funding (grant #2018–01267) for the project titled “Eco-district” and the Swedish Energy Agency funding (46355–1) for the project titled “Solar Districts.”

Conflict of Interests

The authors declare no conflict of interests.

References

Bao, Q., Honda, T., El Ferik, S., Shaukat, M. M., & Yang, M. C. (2017). Understanding the role of visual appeal in consumer preference for residential solar panels. *Renewable Energy*, *113*, 1569–1579. https://doi.org/10.1016/j.renene.2017.07.021

Bomfim, K., & Tavares, F. (2019). Building facade optimization for maximizing the incident solar radiation. *Blucher Design Proceedings*, *7*(2), 171–182. https://doi.org/10.5151/proceedings-ecaadesigradi2019_555

Deville, L., Theristis, M., King, B. H., Chambers, T. L., & Stein, J. S. (2024). Open-source photovoltaic model pipeline validation against well-characterized system data. *Progress in Photovoltaics: Research and Applications*, *32*(5), 291–303. https://doi.org/10.1002/pip.3763

Esfahani, S. K., Karrech, A., Cameron, R., Elchalakani, M., Tenorio, R., & Jerez, F. (2021). Optimizing the solar energy capture of residential roof design in the southern hemisphere through evolutionary algorithm. *Energy and Built Environment*, *2*(4), 406–424. https://doi.org/10.1016/j.enbenv.2020.09.004

Eurostat. (2023). *Share of energy from renewable sources* [Data set]. https://doi.org/10.2908/NRG_IND_REN

Freitas, J. D., Cronemberger, J., Soares, R. M., & Amorim, C. N. (2020). Modeling and assessing BIPV envelopes using parametric Rhinoceros plugins Grasshopper and Ladybug. *Renewable Energy*, *160*, 1468–1479. https://doi.org/10.1016/j.renene.2020.05.137

Holmgren, W., Andersson, K., Hansen, C., robwandrews, Mikofski, M., Jensen, A. R., Lorenzo, A., Krien, U., bmu, Driesse, A., Stark, C., DaCoEx, Sánchez de León Peque, M., Transue, T., Luis, E., kt, Priyadarshi, N., mayudong, Heliolytics, . . . Morgan, A. (2023). *pvlib/pvlib-python: v0.10.3*. Zenodo. https://doi.org/10.5281/ZENODO.10412885

Holmgren, W. F., Hansen, C. W., & Mikofski, M. A. (2018). pvlib python: A python package for modeling solar energy systems. *Journal of Open Source Software*, *3*(29), Article 884. https://doi.org/10.21105/joss.00884

Joint Research Center. (2018). *Implementation plan on positive energy districts*. European Commission. https://setis.ec.europa.eu/implementing-actions/positive-energy-districts_en

Kalogirou, S. A. (2013). Building integration of solar renewable energy systems towards zero or nearly zero energy buildings. *International Journal of Low-Carbon Technologies*, *10*, 379–385. https://doi.org/10.1093/ijlct/ctt071

Kastner, P., & Dogan, T. (2021). Eddy3D: A toolkit for decoupled outdoor thermal comfort simulations in urban areas. *Building and Environment*, *212*, Article 108639. https://doi.org/10.1016/j.buildenv.2021.108639

Nejat, P., Jomehzadeh, F., Taheri, M. M., Gohari, M., & Abd. Majid, M. Z. (2015). A global review of energy consumption, CO_2 emissions and policy in the residential sector (with an overview of the top ten CO_2 emitting countries). *Renewable and Sustainable Energy Reviews*, *43*, 843–862. https://doi.org/10.1016/j.rser.2014.11.066

O'Hegarty, R., Kinnane, O., & McCormack, S. J. (2016). Review and analysis of solar thermal facades. *Solar Energy*, *135*, 408–422. https://doi.org/10.1016/j.solener.2016.06.006

OpenStreetMap. (2017). *Planet OSM*. https://planet.osm.org

Ricci, A., Kalkman, I., Blocken, B., Burlando, M., & Repetto, M. P. (2020). Impact of turbulence models and roughness height in 3D steady RANS simulations of wind flow in an urban environment. *Building and Environment*, *171*, Article 106617. https://doi.org/10.1016/j.buildenv.2019.106617

Rizzo, A., Ekelund, B., Bergström, J., & Ek, K. (2020). Participatory design as a tool to create resourceful communities in Sweden. In C. Smaniotto Costa, M. Mačiulienė, M. Menezes, & B. Goličnik Marušić (Eds.), *Co-creation of public open places: Practice – reflection – learning* (pp. 95–107). Lusófona University Press. https://doi.org/10.24140/2020-sct-vol.4-1.6

Rossi, A. (2021). *Wasp v0.5.008: Discrete design for Grasshopper*. GitHub. https://github.com/ar0551/Wasp

Savvides, A., Vassiliades, C., Lau, K., & Rizzo, A. (2024). Examining user thermal comfort in spaces between buildings: Exploring parametric solutions for BIPVs for Luleå, Sweden, and Limassol, Cyprus. *Energy Reports*, *11*, 5235–5251. https://doi.org/10.1016/j.egyr.2024.04.066

SCB. (2021). *Statistiska tätorter 2020, befolkning, landareal, befolkningstäthet*. www.scb.se/MI0810

Shekar, V., Caló, A., & Pongrácz, E. (2023). Experiences from seasonal Arctic solar photovoltaics (PV) generation—An empirical data analysis from a research infrastructure in Northern Finland. *Renewable Energy*, *217*, Article 119162. https://doi.org/10.1016/j.renene.2023.119162

Shirazi, A. M., Zomorodian, Z. S., & Tahsildoost, M. (2019). Techno-economic BIPV evaluation method in urban areas. *Renewable Energy*, *143*, 1235–1246. https://doi.org/10.1016/j.renene.2019.05.105

Swedish Energy Agency. (2020). *Energy in Sweden 2020: An overview*. https://energimyndigheten.a-w2m.se/FolderContents.mvc/Download?ResourceId=174155

United Nations. (2023). *The Sustainable Development Goals report 2023: Special edition*. https://desapublications.un.org/publications/sustainable-development-goals-report-2023-special-edition

Vassiliades, C., Lau, K., Moiseos, R., Buonomano, A., Savvides, A., & Rizzo, A. (2023). A climate sensitive design approach to BIPV: Investigating the nexus between solar energy and thermal comfort in cities in Sweden and Cyprus. *Building and Environment*, *243*, Article 110681. https://doi.org/10.1016/j.buildenv.2023.110681

Vestartas, P., & Rad, A. R. (2021). *NGon*. Zenodo. https://doi.org/10.5281/ZENODO.4550592

Vulkan, A., Kloog, I., Dorman, M., & Erell, E. (2018). Modeling the potential for PV installation in residential buildings in dense urban areas. *Energy and Buildings*, *169*, 97–109. https://doi.org/10.1016/j.enbuild.2018.03.052

Walker, L., Hofer, J., & Schlueter, A. (2019). High-resolution, parametric BIPV and electrical systems modeling and design. *Applied Energy*, *238*, 164–179. https://doi.org/10.1016/j.apenergy.2018.12.088

About the Authors

Max Spett is a PhD candidate at the Architecture group at Luleå University of Technology, Sweden. He holds a Master of Architecture degree from the Royal Institute of Technology, Stockholm. Max's research lies at the intersection between energy efficiency, digitality, and history. He has researched automation strategies for microclimate model generation and is currently investigating the role of aesthetics in automated timber component manufacturing processes.

Kevin Lau, an urban climatologist with 15 years of experience, specializes in climate-sensitive urban planning and design. His research focuses on the relationship between the built environment and urban climate, particularly human thermal comfort outdoors. He explores the interplay between the built environment, climate, and health. Kevin has led interdisciplinary projects for government, NGOs, and private sectors, and is a member of the WMO Expert Network on various commissions.

Agatino Rizzo is the chaired professor of architecture at Luleå University of Technology (LTU) in Sweden. In this university he leads a research group of 25 people focusing on the climate transition in cities, urban living labs, and climate-sensitive design/planning. His research has been funded by, among others, Qatar QNRF, EU Horizon, Swedish Energy Agency, Formas, and Vinnova.